Exciton–LO-phonon couplings in spherical semiconductor microcrystallites

Shintaro Nomura and Takayoshi Kobayashi
Department of Physics, University of Tokyo, Hongo, Bunkyo-ku, Tokyo, Japan
(Received 2 May 1991; revised manuscript received 5 August 1991)

Exciton–LO-phonon couplings in CdS_xSe_{1-x} semiconductor microcrystallites ($x=0.12\pm0.05$) are investigated by measuring the temperature dependence of the width and energy of excitons by electroabsorption. The LO phonons are shown semiquantitatively to contribute to the experimentally obtained temperaure dependencies of the width and energy of excitons. The dependence of the coupling constant (the Huang-Rhys parameter) on the radius of microcrystallites is calculated for CdSe and GaAs microcrystallites. The phonon confinement effects are considered with "free-standing" and "rigid"-boundary conditions. As for the exciton state, nonparabolicity of the conduction band and the valence-band mixing are considered in order to obtain a precise exciton wave function, which is crucially important in calculating the Huang-Rhys parameter in a microcrystallite. The exciton–confined-optical-phonon interaction Hamiltonian is constructed for a microcrystallite. It is found that the Huang-Rhys parameters have a minimum at a radius of 70 Å for CdSe and 270 Å for GaAs microcrystallites. The size dependence of the Huang-Rhys parameter is also calculated for a microcrystallite with an extra charge at the spherical-particle center. The lowest $(s,S_{3/2})$ state in the trapped state is found to have small transition probability and g values of 1 in CdSe ($R=30$ Å) and 0.01 in GaAs ($R=100$ Å). The higher states are found to have larger transition probability and g values of 0.7 in CdSe ($R=30$ Å) and 0.01 in GaAs ($R=100$ Å). These results suggest that large g values observed experimentally in CdS and CdSe microcrystallites originate from extrinsic effects such as the presence of charged point defects inside the microcrystallite.

I. INTRODUCTION

The size quantization of electron and hole states in semiconductor microcrystallites[1,2] has been extensively investigated.[3–8] Their density of states is known to be transformed from the continuum states of bulk semiconductors to discrete states by confinement and exhibit so-called blueshift of the transition energy from the ground state to the lowest excited states. Because of this size-quantization effect, the oscillator strength is concentrated on discrete states and microcrystallites are promising materials for large optical nonlinearities.[9–13] In attaining these large optical nonlinearities, the spectral width of an exciton plays an important role.[14] If the oscillator strength is distributed over a broad spectral region, the potential superiority of microcrystallites over other low-dimensional materials such as quantum-well structures is seriously diminished. The intrinsic width is introduced by the exciton-phonon coupling. The inhomogeneous width that originates from the distribution in the size of microcrystallites is expected to be decreased with progress in sample-preparation techniques. Katsikas *et al.*[15] have succeeded in achieving a reduction of the inhomogeneous width in the absorption spectra of CdS microcrystallites by applying electrophoresis to select the size of microcrystallites and obtain samples with a standard deviation of 7% in radius. Although they could observe several quantized states in the second derivatives of the absorption spectra, the absorption spectra were as broad as the conventional microcrystallites, indicating the dominance of the homogeneous width over the inhomogeneous width. The exciton-phonon coupling in microcrystallites has been studied by Rosseti, Nakahara, and Brus by use of resonance Raman spectroscopy.[16] They observed the resonance Raman spectrum of LO phonons, which were found to be similar to the bulk spectrum. Recently, couplings to LO phonons through the Fröhlich interaction have been reported by several groups[17–21] by the resonance Raman spectroscopy,[17] spectral hole burning,[18,19] and photoluminescence studies.[19–21] It has been suggested experimentally that a microcrystallite of smaller radius exhibits larger couplings to LO phonons because of the increase in couplings to higher frequency phonons as the wave function is confined in real space.

However, these experimental results contradict the theoretical estimation of the reduction of the couplings to LO phonons in microcrystallites by Schmitt-Rink, Miller, and Chemla.[14] Their estimation was carried out for an extremely confined region that the wave functions for an electron and a hole are identical because of the dominant kinetic energy. In this case, the exciton–LO-phonon coupling constant proportional to the difference in the Fourier transformed wave functions between an electron and a hole completely vanishes. In the bulk, because the exciton formation is attained by the Coulomb interaction, the extent of the wave function in real space is determined by the effective masses. Therefore, a net coupling to LO phonons remains because of the difference in the effective masses between an electron and a hole. The microcrystallites investigated in the present paper are inbetween these two extremes.

The confinement strength can be classified in two ways:

One is associated with the Coulomb interaction and the other is with the LO-phonon energy. The case when the confinement energy is larger than the Coulomb energy between an electron and a hole is called the strong confinement region, while the case when the former is smaller than the latter is called the weak confinement region. There is also an intermediate confinement region, where the confinement energy of an electron is larger but that of a hole is smaller than the Coulomb energy. Here we call an electron-hole pair interacting with the Coulomb interaction an exciton. As far as the interaction with LO phonons is concerned, the other classification is useful. In this case, the confinement energy is compared with the phonon energy. When the former is larger than the latter, the transitions of the electronic states by phonons are small, and the system can be treated in first order with the independent-phonon model.[22] On the contrary, when the former is smaller than the latter, the transitions of the electronic states become important and the system approaches the bulk semiconductor with continuum energy bands. In this paper, we consider the case where an electron and a hole are in the strong or intermediate confinement region, while the electron-phonon system can be treated with the independent-phonon model.

A theoretical investigation of electron-phonon couplings in microcrystallites was recently given by Klein *et al.*[23] They assumed that a hole is localized at the center of a sphere and used a δ function for the state density of a hole. They also assumed a spherical Bessel function for an electron, which is valid only in the strong confinement region. They concluded that the coupling constant is size independent. However, as they recognized, their model was not very realistic. Here we present calculations with more precise wave functions by taking into account the nonparabolicity of the conduction band and the valence-band mixing and investigate the size dependence of the coupling constant accurately.

In Sec. II, we describe experimental results, and in Sec. III, the experimental results of the temperature dependence of the exciton energy and width are investigated with the use of the modulation spectroscopy of absorption. This technique has been shown in our previous papers[24,25] to be effective in the determination of the energy and width of excitons in microcrystallites. The experimentally obtained data are discussed in terms of the LO phonons in Secs. IV A and IV B. In Sec. IV C, the temperature dependencies of the shift and broadening by the external electric field are discussed. In Sec. V the exciton–LO-phonon coupling constant (the Huang-Rhys parameter[26]) is investigated theoretically with the Fröhlich interaction. The calculation scheme is similar to those for bulk,[27] quantum wells,[28–30] or quantum wires[31] except that the independent-boson model is assumed. The confined phonon modes and the interface mode in a spherical microcrystallite are investigated in Secs. V B and V C. The size dependence of the coupling strength is reflected through the wave function for the exciton. For the purpose of calculation of the exciton–LO-phonon coupling, it is crucially important to obtain the wave function precisely. Therefore we take into consideration nonparabolicity of the conduction band and the valence-band mixing. The exciton state is constructed in Sec. V D and results and discussions of the theoretical calculations are given in Sec. V E. Finally conclusions of this work are given in Sec. VI.

II. EXPERIMENTAL

The samples used were CdS_xSe_{1-x} ($x=0.12\pm0.05$) microcrystallites, of which details are given in a previous paper.[24] The average radii of the microcrystallites were between 50.5- and 17.5 Å. A pair of aluminum electrodes with 0.40- and 0.48-mm gap were evaporated on the surface of the sample plates of 50.5- and 17.5-Å microcrystallites, respectively, and sinusoidal waves with 1.0 and 1.4 kV and frequency (f) of 500 Hz were applied, respectively. The linear dilation constant of the glass is 8×10^{-6} K^{-1},[32] which is small enough to be assumed that the electric field applied to the sample was constant throughout 15–300 K. The samples had higher resistance than 20 MΩ, and any thermal effects were eliminated.

The temperature of the samples in a continuous-flow helium cryostat (Oxford Instrument, CF1100) was stabilized by conduction through a copper sample holder within 0.1 K in the range 15–293 K. The sample room of the cryostat was evacuated to less than 3×10^{-5} Torr to avoid discharges between electrodes. After the temperature was set at 15 K and it was kept for longer than 90 min, the temperature of the samples was ascertained by the peak position of the transmittance change spectra. The samples of doped glasses were attached to Bakelite plates converged with aluminum films except areas close to the electrodes resulting in better thermal conductivity. Any detectable temperature rise of the samples was eliminated by the small illuminated part of the samples, which was 1×4 mm^2 together at a low power density of the probe light from an incandescent lamp that passed through a monochromator.

The transmittance change of the samples induced by an external electric field was measured with a lock-in amplifier. A high signal-to-noise ratio was maintained by stabilizing a power supply to the incandescent lamp and also by wide entrance and exit slits of the monochromator with a resolution of 2–3 meV.

III. EXPERIMENTAL RESULTS

The absorption spectra and the absorbance-change spectra of the samples are shown in Figs. 1 and 2, respectively. In our previous paper, we found two identical structures in 1.9–2.0 eV and 2.3–2.4 eV, which originated from the spin-orbit split of the valence bands. In the present paper, we shall focus on the structure at 1.9–2.0 eV. In both the absorption and the absorbance-change spectra, the exciton peak was seen to shift toward lower energy as the temperature was increased. Little change in the line shapes was observed.

The absorbance-change spectra were analyzed with a Gaussian distribution for a lowest exciton and with parabolic bands for an unresolved ensemble of higher exciton

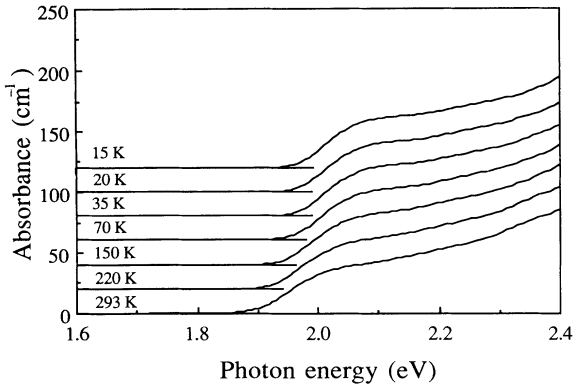

FIG. 1. The absorption spectra of 17.5-Å microcrystallites. The zero points are shifted as shown by the solid lines.

states being assumed.[24] From the fits, the energy positions and the widths of the excitons were precisely determined, because only the lowest exciton was sensitive to the external electric field. Higher excitons were not, probably because of the large widths of the higher excited states, which were due to rapid nonradiative transitions to lower states and stronger couplings to LO phonons. The obtained temperature dependence of the exciton energy is shown in Fig. 3. The bulk band gap from Ref. 30 is also depicted. In the temperature region lower than 50 K, the exciton energy is almost constant, and at temperatures higher than 70 K, the exciton energy decreases linearly with the temperature. This behavior is similar to the temperature dependence of the band gap of bulk diatomic semiconductors, which suggests the involvement of the optical phonons. The first derivatives of the exciton energy by the temperature above 70 K were

$$\frac{dE}{dT} = -3.1\times10^{-4}\ \text{eV K}^{-1} \quad (R = 50.5\ \text{Å for 70–290 K}) \quad (1)$$

and

$$\frac{dE}{dT} = -2.6\times10^{-4}\ \text{eV K}^{-1} \quad (R = 17.5\ \text{Å for 70–293 K}) . \quad (2)$$

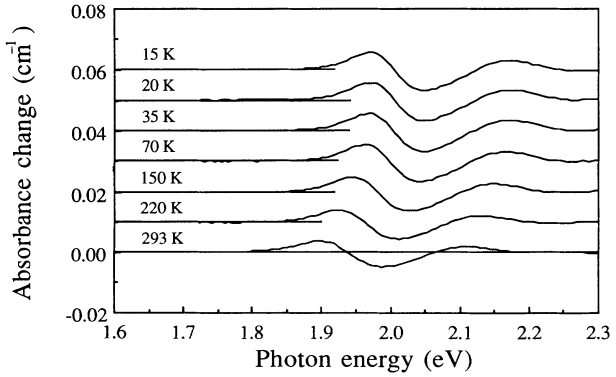

FIG. 2. The absorption-change spectra of 17.5-Å microcrystallites. The zero points are shifted as shown by the solid lines.

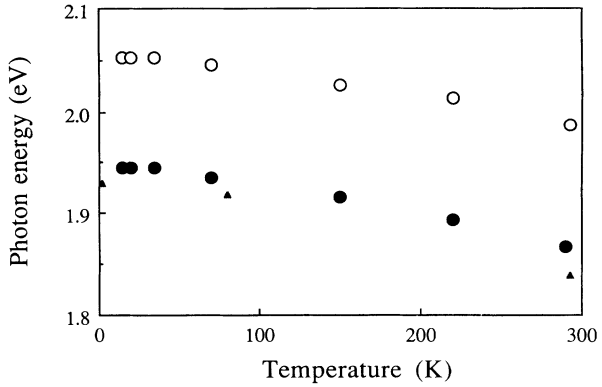

FIG. 3. The temperature dependence of the exciton energy of microcrystallites of 17.5 Å radius (open circles) and 50.5 Å radius (closed circles). The temperature dependence of the bulk band gap is also depicted (Ref. 35) (triangles).

The decrease in the derivative with radius is due to the quantum confinement effects, as will be discussed later.

In Fig. 4, the temperature dependence of the full width at half maximum of the exciton is shown. The deviation of the measurement in the width is about 3 meV. This width includes both the inhomogeneous and the homogeneous width. Although the former is dominant in our samples, the latter plays an important role in the temperature dependence about 70 K.

The Stark shifts and the broadenings induced by the external electric field between 15 and 293 K are shown in Figs. 5 and 6. The values are normalized at 15 K. The errors in the broadenings and the shifts are estimated to be 10% and 20%, respectively. These errors are mainly due to arbitrary parameters for the exciton line shapes fitted to a Gaussian distribution. No significant temperature dependence is seen in both the shifts and the broadenings. This suggests that the observed absorbance changes are mainly electronic in origin, and the phonons play little role. These results will be discussed in the following sections.

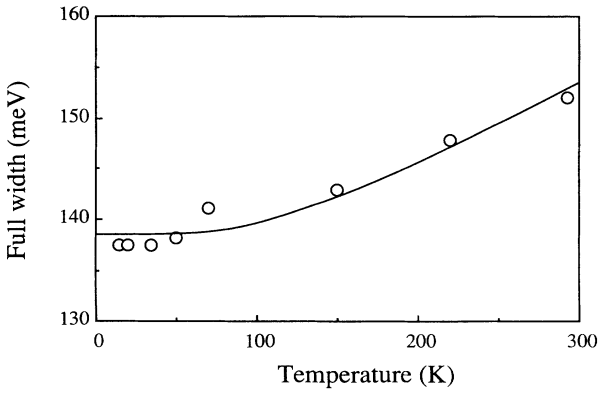

FIG. 4. The temperature dependence of the full widths at half maximum of the exciton of microcrystallites of 17.5 Å radius (open circles). The solid curve is the best fitted curve assuming the LO-phonon energy of 28 meV.

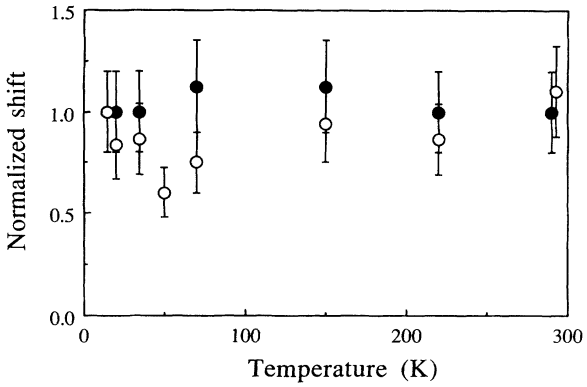

FIG. 5. The temperature dependence of the Stark shift of the exciton energy by applying the external electric field of microcrystallites of 17.5 Å radius (open circles) and 50.5 Å radius (closed circles). The values are normalized at 15 K.

IV. DISCUSSION OF THE EXPERIMENTAL RESULTS

A. Temperature dependence of the exciton energy

Temperature dependence of the band gap of bulk semiconductors was investigated in the 1950s. First, it was considered in terms of the temperature-dependent dilation of the lattice,[33] but the calculated energy shift of the band gap was smaller than the experimental values in polar crystals. Later, the remaining shift was explained by the band-gap renormalization by LO phonons. The electrons in a conduction band and holes in valence bands are scattered by the interaction with LO phonons into continuum bands. From second-order perturbation theory, the band gap is decreased as[34]

$$\Delta E_g = -\frac{f_0^2}{4\pi(\hbar\omega)^{1/2}}\left[\left[\frac{2m_1^*}{\hbar^2}\right]^{1/2} + \left[\frac{2m_2^*}{\hbar^2}\right]^{1/2}\right][n(T)+1]\,. \quad (3)$$

Here, E_g and f_0 are the bulk band-gap energy and the Fröhlich interaction coupling constant, respectively, m_1^* and m_2^* are the effective masses of an electron and a hole, respectively, and $n(T)$ is the Bose distribution function at the temperature T. About 75% of the decrease in the band-gap energy was attributed to interaction with the LO phonons, and the remaining to the dilation of the lattice.

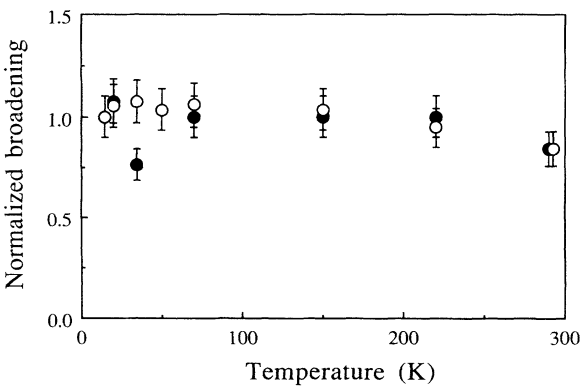

FIG. 6. The temperature dependence of the broadening of the exciton energy by applying the external electric field of microcrystallites of 17.5 Å radius (open circles) and 50.5 Å radius (closed circles). The values are normalized at 15 K.

The experimental value of dE/dT of the band-gap energy of CdS_xSe_{1-x} obtained from the values of bulk CdS and CdSe (Ref. 35) is

$$\frac{dE}{dT} = -3.6\times10^{-4}\ \text{eV K}^{-1}$$

(for bulk CdS_xSe_{1-x}, 77–300 K). (4)

The results represented by (1), (2), and (4) give the conclusion that as the confinement becomes stronger, dE/dT becomes smaller.

There are several causes to be considered to explain the temperature dependence. First, let us consider the temperature dependence of the confinement energy by the lattice dilation. The lattice constants of CdS_xSe_{1-x} are calculated from the values of CdS and CdSe in Ref. 35 as 4.284 Å at 4.2 K and 4.290 Å at 300 K. The calculated contribution to dE/dT is smaller than 1×10^{-6} eV K^{-1} and can be neglected. Second, the temperature dependence of the static dielectric constants is considered: The specific dielectric constant of CdS_xSe_{1-x} is 9.17 at 100 K and 9.64 at 300 K.[35] This causes the decrease in the Coulomb energy of an exciton in a microcrystallite by 5% when the sample temperature is changed from 100 to 300 K. The experimental values of the Coulomb energy in the microcrystallites are not known and only the confinement energies are experimentally available. Therefore, we estimate the Coulomb energy to be 21 and 31 meV for 50.5- and 17.5-Å microcrystallites, respectively, from the ratio of the confinement energy to the Coulomb energy term in the theoretical calculations.[5,25] Then, the contributions to dE/dT are 5.3×10^{-6} and 7.8×10^{-6} eV K^{-1} for 50.5- and 17.5-Å microcrystallites, respectively, which are two orders smaller than the values in (1), (2), and (4). Third, the temperature dependence of the effective masses is considered. The effective mass was found to decrease with increase in temperature both theoretically[36] and experimentally.[35] This was attributed to the lattice dilation. The experimental value of the temperature dependence of the effective mass of CdSe is not known, which we assumed to be similar to that of CdS. Using the values in Ref. 35 the effective mass decreases by 8% by changing temperature from 15 to 300 K. When the effective mass becomes smaller, the kinetic energy term proportional to $\hbar^2/2m^*$ becomes larger. The increase in this term is calculated using the experimentally obtained confinement energy. Then dE/dT is calculated as 1.5×10^{-5} eV K^{-1} and 4.9×10^{-5} eV K^{-1} for 50.5- and 17.5-Å microcrystallites, respectively. This effect is not negligible especially in small microcrystallites but still smaller than the experimental results.

Therefore, the remaining origin of the temperature dependence to be considered is the change in the self-energy due to the interaction of excitons with the LO phonons. Before discussing this theory, we shall consider the temperature dependence of the width in the following section.

B. Temperature dependence of the exciton width

The temperature dependence of the width of excitons in microcrystallites is also to be discussed by taking the exciton–LO-phonon interaction into account. Voigt, Spielgelberg, and Senoner observed only little temperature dependence in the absorption spectra of CdSe microcrystallites,[37] which was attributed to the lack of ionization of excitons into free electrons and holes. Evidently, this is also the case for our samples as seen in the absorption spectra in Fig. 5. Several different origins contribute to the observed spectral widths of the excitons. The first is the inhomogeneous width due to the size distribution in the microcrystallites, the second is the lifetime width due to the recombination with the surface charges or the trapping to the surface states, and the third and the fourth are the widths due to the interaction of the excitons with longitudinal acoustic (LA) phonons and longitudinal optical (LO) phonons, respectively. The widths due to the inhomogeneity and the surface charges or states are considered to be temperature independent. The LO-phonon frequency in microcrystallites was measured by Rossetti, Nakahara, and Brus[16] by means of the resonance Raman spectroscopy and was found to be identical with the bulk phonon frequency. Therefore, the solid curve in Fig. 4 is obtained by using the LO-phonon energy in CdS_xSe_{1-x} microcrystallites calculated to be 28 meV by interpolating between those of CdS and CdSe in Ref. 35.

The increasing and decreasing contributions of longitudinal LA and LO phonons with decreasing microcrystallites size have been estimated by Schmitt-Rink, Miller, and Chemla.[14] The linear dependence of the width on the temperature below the LO-phonon energy is expected to be observed because of the coupling to LA phonons following their estimations. Contrary to this, no distinct temperature dependence is seen below 50 K as shown in Fig. 4. This does not necessarily mean that there are no LA phonons contributing to the width. The experimental results show that even though the coupling to LA phonons increase in microcrystallites, the contribution of LA phonons is still smaller than that of LO phonons, and LA phonons are less important in the temperature dependence in the region observed in the present experiments. In the temperature region less than about 30 K, the interaction with LA phonons is important. To observe the enhancement of the interaction with LA phonons, it is necessary to measure the width with higher resolution and at lower temperature than in the present experiment.

The smaller contribution of LA phonons to the interaction with excitons in microcrystallites comes from the persistent interaction with LO phonons in a strongly confined region. The widths due to the coupling to LO phonons divided by the Bose factor are 30 and 29 meV for 50.5- and 17.5-Å microcrystallites, respectively, by fitting the experimentally obtained widths to theoretical curves assuming the LO-phonon energy of 28 meV. The width divided by the Bose factor of bulk CdSe is 106 meV.[37] Clearly, the confinement effect as pointed out by Schmitt-Rink, Miller, and Chemla is observed.[14] This reduction in the exciton width reflects the quantization of the electron states in microcrystallites that there are no free electron and hole continuum states for excitons to be ionized. However, it is still non-negligible and plays an important role in the temperature dependence higher than 70 K through phonon-assisted transitions of excitons although the width by LO phonons is greatly reduced.

C. Temperature dependence of the shift and broadening by the external electric field

The Stark shift in a confined system was investigated by Miller and others.[38,39] They observed the red shift of the exciton peaks up to very high field and called the shift a quantum confined Stark effect. The observed shift in the present experiment is similar to this. Figure 5 shows no temperature dependence of the shift in agreement with their theory and ours.[25] The broadening is also observed. Hache, Ricard, and Flytzanis[40] claimed that the electroabsorption spectra can be explained with shifts of the elementary absorption peaks and appearance of additional transitions due to the mixing of unperturbed states. We do not follow their interpretation because (1) the observed line shapes can be better fit by the shift and broadening of Gaussian peaks representing excitons than by the shift of excitons and the emergence of these additional states, and (2) the width obtained by this fit shows the temperature dependence as shown in Fig. 4, which supports our interpretation, but cannot be explained by theirs. Moreover, these states failed to be observed under the introduction of the external electric field. The lack of additional states is explained by the modification of the selection rule with the introduction of the Coulomb interaction and the valence-band mixing, and partly by the lower symmetry of the microcrystallites rather than a perfect sphere due to imperfections. Lower symmetry allows the forbidden states in the sphere to appear without the external electric field. The widths of such excited states were large and the change in their oscillator strength was not observable.

There is no clear temperature dependence in the broadening spectra as shown in Fig. 4. This suggests that phonons are not involved in the broadening by the external electric field. Here, the effects of the surface have to be considered. Wang *et al.*[41] showed theoretically that surface charges are responsible for the width of exciton peaks in the intermediate confinement region where the radius of a microcrystallite is larger than the electron or hole effective Bohr radius but smaller than the exciton Bohr radius. The effect of the surface to the width of excitons is also shown experimentally by Alivisatos *et al.*[42] They observed the narrowing of exciton peaks after subduing samples to reduce the number of defects. This indicates the lifetime width due to the recombination rate with surface charges also contributes to the obesrved broadening.

V. THEORETICAL CONSIDERATIONS

A. Comparison of the exciton–LO-phonon interaction in bulk and in microcrystallites

The temperature dependencies of both the exciton energy and width suggest couplings to LO phonons. How-

ever, interaction with the LO phonons in microcrystallites differs from that in bulk. First, all the states in the microcrystallites are discrete. In bulk there is a continuum state as a final state of scatterings, but in microcrystallites, there is no such state and scatterings can occur in first order only when the energy separations of the discrete states coincide with the LO-phonon energy. Second, as pointed out by Schmitt-Rink, Miller, and Chemla, the exciton–LO-phonon interaction is completely quenched in microcrystallites of infinite barriers because of the complete cancellation of the "polaron clouds" of an electron and a hole.[14] In this section we attempt to briefly discuss the bulk-phonon–exciton interaction before we construct the confined-phonon–exciton interaction Hamiltonian.

The interaction Hamiltonian for bulk-phonon modes[37] is

$$H_{\text{ex-ph}}=\sum_{\substack{q\\ \lambda,\mu}}\frac{1}{V_0^{1/2}}\frac{f_0}{q}v_{\lambda\mu}(q)B_\lambda^\dagger B_\mu[a(q)+a^\dagger(-q)]\ , \tag{5}$$

where

$$v_{\lambda\mu}(\mathbf{k})=\int d^3r_1 d^3r_2\ \Psi_\lambda^*\Psi_\mu[\exp(i\mathbf{k}\cdot\mathbf{r}_2)-\exp(i\mathbf{k}\cdot\mathbf{r}_1)]\ , \tag{6}$$

$B^\dagger$ and $a^\dagger$ are the exciton and phonon creation operators, respectively, λ and μ represent the quantum numbers of exciton states, V_0 is the volume for the quantization, and r_1 and r_2 are the coordinates of an electron and a hole. We call the electron-hole pair states in microcrystallites excitons, although the confinement is attained by the confining potential rather than the Coulomb potential in the case of strong confinement. There are two limiting cases to be considered. The first one is the case when the phonon energy ($\hbar\omega_{\text{LO}}$) is smaller than the energy separation of the electronic (excitonic) states. The transitions of the electronic states by the interaction with phonons can be ignored in first order. In this case, the independent-boson model[22] that describes localized electronic states well is applicable. The Hamiltonian can be exactly diagonalized and the absorption coefficient can be given by

$$\begin{aligned}\alpha(\hbar\omega)=\alpha_0\sum_{\lambda,m}&\exp[-g_\lambda(2n+1)]\\&\times I_m\{2g_\lambda[n(n+1)]^{1/2}\}\exp\left[\frac{m\hbar\omega_{\text{LO}}}{2k_BT}\right]\\&\times\delta(\hbar\omega-E_\lambda+g_\lambda\hbar\omega_{\text{LO}}-m\hbar\omega_{\text{LO}})\ ,\end{aligned} \tag{7}$$

where α_0 is an absorption coefficient without any phonon interaction and I_m is the modified Bessel function, and the Huang-Rhys parameter g_λ is given as

$$g_\lambda=\frac{f_0^2}{(2\pi)^3}\int d^3k\frac{1}{k^2}\frac{|v_{\lambda\lambda}(k)|^2}{(\hbar\omega_{\text{LO}})^2}\ . \tag{8}$$

The second case is applicable for a system that has energy bands such as bulk semiconductors and quantum wells, where $\hbar\omega_{\text{LO}}$ is larger than energy separations. In this case, the final state λ is not necessarily equal to μ and scatterings to continuum states or to higher excited states become important. Since elaborate approximations are necessary to diagonalize the Hamiltonian,[43] the full width at half maximum (FWHM) is obtained conventionally from Fermi's golden rules as[27]

$$\begin{aligned}\Gamma_{\text{LO}}=\frac{n(T)f_0^2}{(2\pi)^2}\int d^3q\sum_\lambda q^{-2}|v_{\lambda,\mu}(q)|^2\\\times\delta(E_\lambda(q)-E_\mu(0)-\hbar\omega_{\text{LO}})\ .\end{aligned} \tag{9}$$

In the following sections, we will consider the couplings to LO phonons in the independent-boson model.

B. The confined-LO-phonon modes

The confinement of the phonon modes is considered within the continuum model.[44] This model gives good approximation when the radius is sufficiently larger than the lattice constant. The displacement of ions (u) satisfies the equation

$$(\nabla^2+k^2)\mathbf{u}=\mathbf{0}\ , \tag{10}$$

where k is the mode frequency of the phonons. We find the solution of the equation, which is longitudinal ($\nabla\times u=0$) and regular at $r=0$ in the spherical coordinate (r,θ,φ). Two types of boundary conditions are considered; one is the case where there is no pressure at the surface, i.e.,

$$\nabla\cdot u|_{r=R}=0\ , \tag{11}$$

and the other is the case where there is no displacement normal to the surface, i.e.,

$$u_r|_{r=R}=0\ . \tag{12}$$

We will call the first and second cases free-standing and rigid boundary conditions. The former is appropriate for a microcrystallite embedded in a polymer film, and the latter for a microcrystallite embedded in a glass matrix. The solution of (10) is given as

$$\begin{aligned}u_r&=C_{nl}j_l'(q_{ln}r)Y_{lm}(\theta,\varphi)\ ,\\u_\theta&=C_{nl}\frac{j_l(q_{ln}r)}{q_{ln}r}\frac{\partial}{\partial\theta}Y_{lm}(\theta,\varphi)\ ,\\u_\varphi&=C_{nl}\frac{j_l(q_{ln}r)}{q_{ln}r}\frac{im}{\sin\theta}Y_{lm}(\theta,\varphi)\ ,\end{aligned} \tag{13}$$

where C_{nl} is the amplitude of mode n,l. The assumption that the polarization of the ions is proportional to the displacement gives

$$E=-\nabla\Phi=-4\pi U\mathbf{u}\ , \tag{14}$$

where

$$U^2=\frac{\rho\omega_{\text{LO}}^2}{4\pi}\left[\frac{1}{\epsilon_\infty}-\frac{1}{\epsilon_0}\right]\ , \tag{15}$$

and ρ is the density of the crystal. The corresponding phonon potential is

$$\Phi=4\pi U\frac{C_{nl}}{q_{ln}}j_l(q_{ln}r)Y_{lm}(\theta,\varphi)\ . \tag{16}$$

From the boundary condition (11) or (12), $q_{ln}R=a_{ln}$ for the free-standing case, and $q_{ln}R=a_{l+1n}$ for the rigid case, respectively, where a_{ln} is the nth zero of the lth order spherical Bessel function j_l. The mode amplitudes C_{nl} are determined such that the energy expectation values of the modes are equal to their eigen energies as

$$x_{nl}^2M=\rho\int \mathbf{u}^*\cdot\mathbf{u}\,dV\ , \tag{17}$$

where M is the reduced mass. x_{nl} is second quantized as

$$x_{nl}=\left[\frac{\hbar}{2\rho V_0\omega_{q_{ln}}}\right]^{1/2}(a_{q_{ln}}+a_{q_{ln}}^{\dagger})\ . \tag{18}$$

Then we finally obtain the interaction Hamiltonian:

$$\begin{aligned}H_{\text{ex-ph}}&=e\int d^3r_1d^3r_2\,\Psi_\lambda^*\Psi_\mu[\Phi(r_2)-\Phi(r_1)]\\&=\sum_{q_{ln}}\frac{f_0}{q_{ln}R^{3/2}}v_{\lambda\mu}(q_{ln})(a_{q_{ln}}+a_{q_{ln}}^{\dagger})\ ,\end{aligned} \tag{19}$$

where

$$v_{\lambda\mu}(q_{ln})=A_{ln}\int d^3r_1\int d^3r_2\,\Psi_\lambda^*\Psi_\mu[j_l(q_{ln}r_2)Y_{lm}(\theta_2,\varphi_2)-j_l(q_{ln}r_1)Y_{lm}(\theta_1,\varphi_1)]\ , \tag{20}$$

and

$$A_{ln}=\begin{cases}\left[\left(\frac{1}{\sqrt{2}}j_{l+1}(q_{ln}R)\right)\right]^{-1} & \text{(for free-standing boundary)}\\ \left[\frac{1}{2}\left[1-\frac{l^2}{(q_{ln}R)^2}\right][j_l(q_{ln}R)]^2\right]^{-1/2} & \text{(for rigid boundary).}\end{cases}$$

This is just the equivalent of substitution of the spherical wave $j_l(qr)Y_{lm}(\theta,\varphi)$ for the plane wave $\exp(i\mathbf{q}\cdot\mathbf{r})$ in the exciton-bulk-phonon interaction Hamiltonian of (6). Now since the wave vector is quantized because of the confinement, the Huang-Rhys parameter is obtained by substituting summation for the integration in (8) as

$$\begin{aligned}g_\lambda&=\sum_{q_{ln}}g_{\lambda,q_{ln}}\\&=\frac{f_0^2}{R^3}\sum_{q_{ln}}\frac{1}{q_{ln}^2}\frac{|v_{\lambda\lambda}(q_{ln})|^2}{(\hbar\omega_{\text{LO}})^2}\ .\end{aligned} \tag{21}$$

C. The interface LO-phonon mode

As for the free-standing case, it was shown that there is no interface phonon mode[31] in a quantum wire structure because the phonon potential vanishes at the interface. This also holds true in the case of a microcrystallite. As for the rigid case, we consider the continuity of the phonon potential inside and outside of a microcrystallite and apply the boundary condition that velocity normal to the interface and pressure are continuous.[45] The interface mode is a solution of (10), which decays exponentially on both sides of the interface, and the mode frequency should satisfy the condition

$$\omega\geq\omega_1,\omega_2\ . \tag{22}$$

Then the boundary condition is

$$\frac{|q_2|}{\rho_1v_1^2}\frac{j_l'(i|q_1|R)}{j_l(i|q_l|R)}=\frac{|q_1|}{\rho_2v_2^2}\frac{h_l^{(1)\prime}(i|q_2|R)}{h_l^{(1)}(i|q_2|R)}\ , \tag{23}$$

where $\omega_i\rho_i$, v_i, and q_i are the mode frequency, the density, the sound velocity, and phonon wave vector inside ($i=1$) and outside ($i=2$) of a microcrystallite, respectively. From (22) the only mode frequency allowed is $\omega=\omega_1$ and $q_1=0$. In this case, the radial part of the displacement is always zero. Therefore, there is no longitudinal interface mode for the $l=0$ confined-phonon state. The conditions for the mode frequency, $\omega=\omega_1$ and $q_1=0$, hold true for $l\neq0$ states also. In this case, because the phonon potential for the interface modes have a constant radial part and the angular parts of the wave function for an electron and a hole are identical, the exciton-longitudinal-interface-phonon coupling becomes zero for all l.

D. Exciton states

Since the exciton-LO-phonon coupling constant is proportional to the squared absolute value of the difference in the Fourier transforms of the wave functions for an electron and a hole in the bulk case, it is of essential importance to precisely determine the wave functions for an electron and a hole. For this purpose, the effective-mass approximation with parabolic bands for the conduction and valence bands can cause qualitative errors, because this gives identical wave functions for an electron and a hole when the infinite confining potential is assumed. Therefore, it is necessary to treat a multiband envelope function properly. Here, valence-band mixing is calculated according to Xia's theory,[46] and the nonparabolicity of the conduction band is included by the Kane's $\mathbf{k}\cdot\mathbf{p}$ model.[47] In a spherical approximation,[48] small contribution of terms of cubic or hexagonal symmetry is neglected, and the total angular momentum, $\mathbf{F}=\mathbf{L}+\mathbf{J}$ is a constant of motion, where $\mathbf{L}$ and $\mathbf{J}$ are the angular momenta of the envelop function and the Bloch function corresponding to spin $\frac{3}{2}$, respectively.

The Hamiltonian for the exciton state is

$$H_{\rm ex}=E_c(-i\hbar^2\nabla_1)+\frac{\hbar^2}{2m_0}\gamma_1\left[-\nabla_2^2-\frac{\mu_0}{9}(P_h^{(2)}\cdot J^{(2)})\right]+V_B-\frac{e^2}{\epsilon}\frac{1}{|\mathbf{r}_1-\mathbf{r}_2|}+V_C\ , \tag{24}$$

where

$$V_B=\begin{cases}0, & r_i\le R\\ \infty, & r_i>R\end{cases}$$

and

$$V_C=\begin{cases}0 \text{ (for an exciton state)}\\ \dfrac{e^2}{\epsilon}\left[-\dfrac{1}{r_1}+\dfrac{1}{r_2}\right] \text{ (for a trapped state)}\ .\end{cases}$$

Here, r_i's are the radial coordinates for an electron ($i=1$) and a hole ($i=2$), $P_h^{(2)}$ and $J^{(2)}$ are the second-rank irreducible tensor operators, $E_c(k)$ is the nonparabolic conduction-band dispersion,[49] and

$$\mu_0=\frac{2\gamma_2}{\gamma_1}\ . \tag{25}$$

For GaAs, γ_1 and γ_2 are given as the Luttinger parameters. However, since valence-band parameters do not exist for the wurzite crystals, γ_1 and γ_2 for CdSe are determined as follows. In the wurzite structure, valence bands are known to be strongly nonparabolic in the vicinity of the band minimum.[50] Then we take a polarization averaged effective masses in the energy region of present interest between 0.02 and 0.1 eV, where the dispersion can be approximated well as parabolic. Unlike the zinc-blende-structure case, there is a crystal-field splitting of 39 meV for CdSe between Γ_9 and Γ_7 valence band, but this splitting is smaller than the typical kinetic energy of the hole states and thus neglected for the first approximation. Then γ_1 and γ_2 are determined from the averaged valence-band effective masses as

$$m_{A,B}=\gamma_1(1\mp\mu)\ . \tag{26}$$

We use the Haken potential,[51] and the dielectric constant becomes size dependent as

$$\epsilon(r)=\left[\frac{1}{\epsilon_\infty}-\left[\frac{1}{\epsilon_\infty}-\frac{1}{\epsilon_0}\right]\left[1-\frac{\exp(-r/\rho_{p1})+\exp(-r/\rho_{p2})}{2}\right]\right]^{-1}\ , \tag{27}$$

where

$$\rho_{pi}=\left[\frac{\hbar}{2m_i\omega_{\rm LO}}\right]^{1/2}\quad(i=1,2)\ . \tag{28}$$

We substitute $r=\langle r\rangle=0.69932R$ in (13) for simplicity,[5] because $\epsilon(r)$ is a slowly varying function of r. The polarization energy due to the difference in the dielectric constants between the microcrystallite and the surrounding matrix is not considered, since this was shown not to change the exciton energy and the wave function significantly.[23] We have also neglected here the penetration of the wave functions outside a microcrystallite because this effect is less important when the nonparabolicity is included and the kinetic energy is reduced.

The exciton wave function has two components labeled by the orbital angular momentum of a hole state $(L,L+2)$ written as

$$\Psi_{ex\lambda}(r_1,r_2)=\sum a_{\lambda ij}\phi_{eiL_1}(r_1)\phi_{hjL_2F}(r_2)\ . \tag{29}$$

Here, λ represents the quantum number of the exciton, i and j denote the principal quantum numbers of conduction and valence bands, respectively. Only hydrogenic states for which $\Delta L=0,\pm2$ are coupled by the spin-orbit term in the Hamiltonian. The wave functions for an electron and a hole state are given by

$$\phi_{eiL_1}(r_1)=\sum_\sigma f_{eiL_1}(r_1)Y_{L_1m_1}(\theta_1,\varphi_1)|S\sigma\rangle \tag{30}$$

and

$$\phi_{hjL_2F=3/2}(r_2)=\sum_{\substack{L=L_2,L_2+2\\ m_1,m_2}} f_{jL}(r_2)Y_{LM_1}(\theta_2,\varphi_2)|J=\tfrac{3}{2}m_2\rangle\times\langle LJ=\tfrac{3}{2}m_1m_2|F=\tfrac{3}{2}F_z\rangle\ , \tag{31}$$

where $f_{eiL_1}(r_1)$ and $f_{hjL_2}(r_2)$ are radial wave functions, Y_{lm} is the spherical harmonic function, $|S\sigma\rangle$ and $|J=\frac{3}{2}m_2\rangle$ are the Bloch function of spin-σ conduction bands and spin-$\frac{3}{2}$ valence bands, respectively, and $\langle LJ=\frac{3}{2}m_1m_2|F=\frac{3}{2}F_z\rangle$ is the Clebsch-Gordan coefficient.

E. Results and discussion

The Huang-Rhys parameter for the exciton state is obtained by substituting the wave function for the exciton (29) into (20) and (21), the results being shown in Figs. 7(a) and 7(b). The material parameters used in the calculations are summarized in Table I. For CdSe we calculate with $\gamma_1^{-1}=0.45$, 0.68, and 1.0 to see the dependence on the hole masses. Phonon modes of bulk and confined phonon with free-standing and rigid boundaries give the same results for couplings to the lowest $(s,S_{3/2})$ exciton state because the lowest exciton couples mainly to the confined-phonon mode with $l=0$ symmetry. It is seen that as the confinement becomes stronger, the couplings of the exciton to LO phonons become stronger for CdSe microcrystallites of $R<70$ Å ($\gamma_1^{-1}=0.68$) and GaAs microcrystallites of $R<270$ Å. This is due to the increase

in the couplings to higher frequency phonons with the reduction in the radius of the microcrystallite, as is clearly shown in Fig. 8, where the Huang-Rhys parameter for $(s,S_{3/2})$ exciton states with the confined-phonon modes in rigid boundary ($g_{q_{l=0n}}$) is depicted against the confined-phonon wave numbers. Here, the nonvanishing coupling constant is obtained only after the introduction of the valence-band mixing, which makes the wave functions for an electron and a hole not identical in the limit of strong confinement.

The Huang-Rhys parameter of the exciton increases with increasing microcrystallites radius of $R > 70$ Å for CdSe and of $R > 270$ Å for GaAs. In this regime, the Coulomb interaction becomes more important and the difference in the envelope functions for an electron and a hole becomes larger by reflecting the difference in the effective masses. As the radius becomes larger, the confinement effects become less important, and $v_{(s,S_{3/2})}$ approaches the value of bulk semiconductors in which the confinement is totally determined by the Coulomb interaction instead of by barriers. The Huang-Rhys parameter of the bulk exciton is calculated in the Appendix as $g=0.38$, 0.79, and 1.4 for CdSe with $m_2^*=0.45$, 0.68, and 1.0, respectively, and $g=0.0079$ for GaAs with $m_2^*=0.146$.

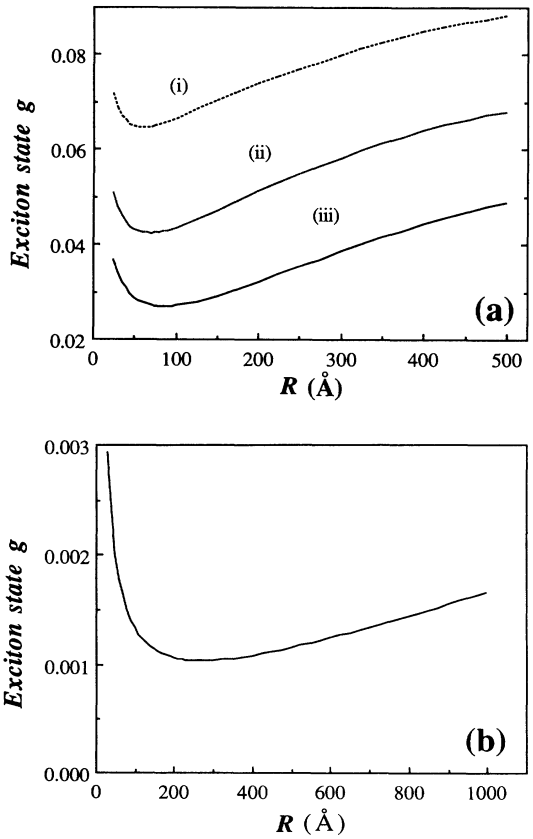

FIG. 7. The calculated size dependence of the Huang-Rhys parameter, g for $(s,S_{3/2})$ exciton states of CdSe (a) with $\gamma_1^{-1}=1.0$ (i), 0.68 (ii), and 0.45 (iii), and for GaAs (b) microcrystallites.

TABLE I. Material parameters used in the calculations. All the parameters are from Ref. 35.

	CdSe	GaAs
Electron mass: m_1^*	0.13	0.0665
Averaged hole mass: m_A	1.7	
m_B	0.43	
Luttinger parameters: γ_1		6.85
γ_2		2.10
Static dielectric constant: ϵ_0	9.56	12.56
Optical dielectric constant: ϵ_∞	6.23	10.9
Band gap: E_G (eV)	1.75	1.424
Spin-orbit splitting energy (eV)	0.42	0.34
LO-phonon frequency: ω_{LO} (s^{-1})	6.3×10^{12}	8.75×10^{12}

The absolute value of g is significantly smaller than experimental results reported by several groups. Bawendi *et al.*[19] observed sharp phonon side bands in photoluminescence excitation spectrum of CdSe microcrystallites of 16 Å radius. By integrating the intensity of the spectrum, they obtained $g=1.4$. The dependence of g on the CdS_xSe_{1-x} microcrystallite size was investigated by Uhrig *et al.*[21] They determined $g\approx0.77$ from a Stokes shift between the absorption and emission for $R=a_B$. These experimental values are much larger than our calculations. In the case of Bawendi *et al.*, the radius is only four times larger than the lattice constant, and their sample is described better as a "cluster" than as a "semiconductor particle." Our calculation can fail to give a good approximation. In the case of Uhrig *et al.*, we cannot explain the results only with intrinsic effects since the correlation between an electron and a hole have already been included without any approximations.

Then the g values are calculated with an extra charge at the center as shown in Fig. 9 for the lowest four $(s,S_{3/2})$ states. An extra charge alters the overlapping of the electron and hole wave function significantly, and thus the optical transition probability f is modified greatly from the exciton states. Here $f=|\langle 0|\mathbf{p}|\Psi_{ex\lambda}\rangle|^2/|p_{cv}|^2$

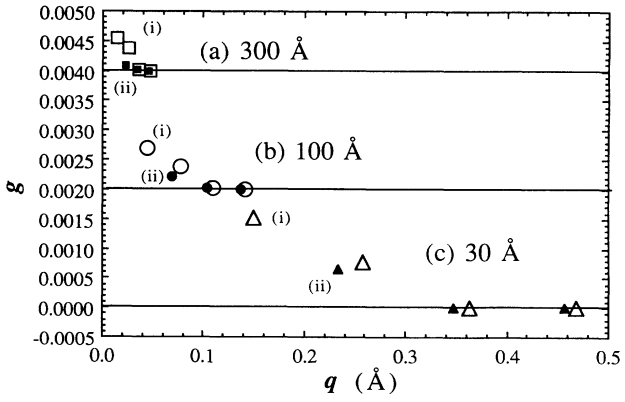

FIG. 8. The Huang-Rhys parameter for $(s,S_{3/2})$ exciton states with the lowest four $l=0$ (i) and $l=2$ (ii) confined phonon modes in rigid boundary ($g_{q_{l=0n}}$) for GaAs microcrystallites of radius of 300 Å (a), 100 Å (b), and 30 Å (c), respectively. The zero points are shifted as shown by the solid lines.

is calculated as shown in Fig. 10, where $|p_{cv}|$ is the momentum matrix element between the conduction band and valence band in the bulk semiconductor. In the exciton states, f is largest in the lowest $(s,S_{3/2})$ state, and the optical transition occurs mainly between the ground and this state. In the trapped states, however, f is redistributed over higher transitions, and for the CdSe, case the lowest $(s,S_{3/2})$ state becomes nearly forbidden. Note here that an extra charge at the center does not change the symmetry of the system and that the redistribution of f is caused by the change in the overlapping integral between the radial wave functions of $(s,S_{3/2})$. Therefore, the size dependence of f in $(s,S_{3/2})$ states shows slightly different behavior in GaAs because the Coulomb interaction is smaller than in CdSe. f is largest in the lowest $(s,S_{3/2})$ state for $R < 110$ Å and is largest in the second lowest $(s,S_{3/2})$ state for $R > 110$ Å.

In CdSe microcrystallites and in GaAs microcrystallites with radius larger than 110 Å, absorption occurs mainly between the ground state and the second to fourth lowest $(s,S_{3/2})$ states in the trapped-state case. Since the absolute values of f and the transition photon energies are very similar to the exciton states, their absorption spectra are nearly identical. The main difference between them is that g is of the order of 0.01 and 0.001 in the exciton states and 1 and 0.01 in the trapped states for CdSe and GaAs microcrystallites, respectively.

Though the lowest $(s,S_{3/2})$ state in the trapped state is practically not detectable in the absorption spectra, it is expected to be found in the emission spectra. As is shown in Fig. 9, it has g larger than that for the absorption where transitions to the states higher or equal to the

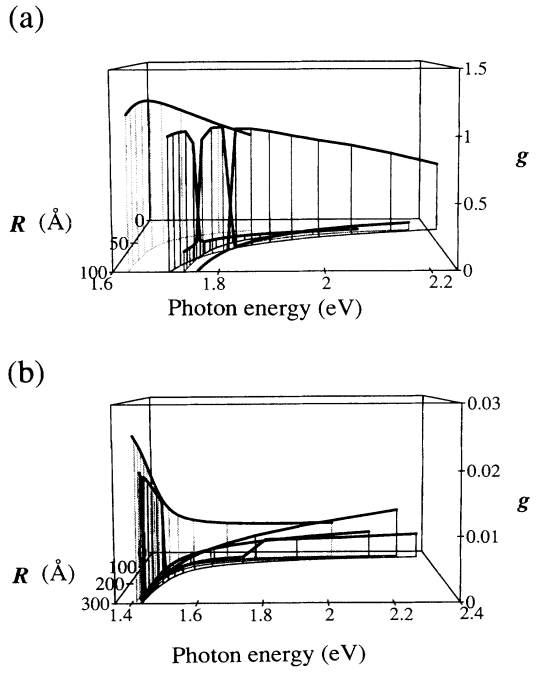

FIG. 9. The calculated size dependence of the Huang-Rhys parameter g for $(s,S_{3/2})$ states with an extra charge at the center of CdSe (a) and GaAs (b) microcrystallites (solid black curves). Gray lines are subsidiary lines to show data points.

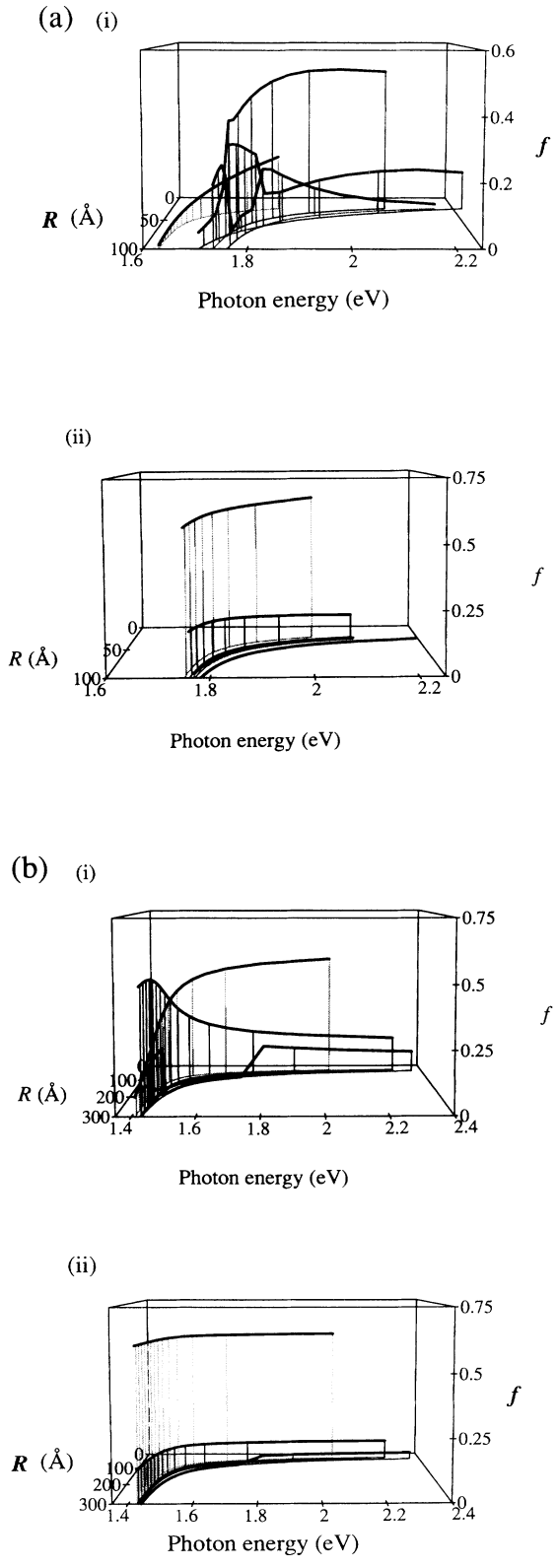

FIG. 10. The calculated optical transition probability, $f=|\langle 0|\mathbf{p}|\Psi_{ex\lambda}\rangle|^2/|p_{cv}|^2$ for $(s,S_{3/2})$ trapped states with an extra charge at the center (i) and exciton states (ii) of CdSe (a) and GaAs (b) microcrystallites (solid black curves). Gray lines are subsidiary lines to show data points.

second lowest state contribute because the lowest $(s,S_{3/2})$ state is more localized in space than the higher states.

VI. CONCLUSIONS

In this paper, the exciton–LO-phonon coupling is investigated both experimentally and theoretically. By utilizing the electroabsorption method, the temperature dependencies of the width and energy of the lowest exciton in CdS_xSe_{1-x} microcrystallites are determined. Both results show that the couplings to LO phonons play an important role although they are smaller than in bulk semiconductors. The exciton–LO-phonon coupling constant, the Huang-Rhys parameter, is calculated for CdSe and GaAs microcrystallites. The phonon confinement effects are considered with free-standing and rigid-boundary conditions. As for the exciton state, nonparabolicity of the conduction band and the valence-band mixing are considered, in order to obtain the exciton wave function precisely, which has crucial importance in calculating the Huang-Rhys parameter in a microcrystallite. The parameter is calculated for an exciton state and a trapped state that has an extra charge at the center of a microcrystallite. It is found that the Huang-Rhys parameter increases with decreasing microcrystallites radius (R) when the radius is smaller than 70 Å for CdSe and 270 Å for GaAs microcrystallites, respectively, and decreases with radius when the radius is larger than 70 Å for CdSe and 270 Å for GaAs microcrystallites. The results are the same for the bulk phonon and confined phonon with free-standing and rigid-boundary conditions because the $(s,S_{3/2})$ exciton couples mainly to a confined phonon with $l=0$ symmetry.

The Huang-Rhys parameter for a microcrystallite with an extra charge at the center is also calculated. The lowest $(s,S_{3/2})$ in the trapped state is found to have a small transition probability and g values of 1 in CdSe ($R=30$ Å) and 0.01 in GaAs ($R=100$ Å). The higher states are found to have larger transition probability and g values of 0.7 in CdSe ($R=30$ Å) and 0.01 in GaAs ($R=100$ Å). These results suggest that large g values observed experimentally originate from the extrinsic effects such as point defects inside of a microcrystallite. It is also shown that a larger g can be observed in the emission from the lowest $(s,S_{3/2})$ state in the trapped state than in the absorption spectra in CdSe and in GaAs with radius larger than 110 Å.

ACKNOWLEDGMENTS

We are grateful to Dr. Uesugi of Nippon Telegraph and Telephone Corporation for providing semiconductor-doped glass samples, and to Meson Science Laboratory, University of Tokyo, for providing CPU time. This work was partly supported by the Ministry of Education, Science, and Culture of Japan under Grant-in-Aid No. 01850003 for the Development of Scientific Research and partly by a Science Grant of Nippon Sheet Glass.

APPENDIX: THE HUANG-RHYS FACTOR FOR A WANNIER EXCITON IN BULK SEMICONDUCTORS

The Huang-Rhys factor is investigated for a free electron and for a localized electron such as color centers,[26] a shallow donor, an exciton bounded to a neutral defect,[52] and an exciton in which a hole is strongly localized.[53] However, for a Wannier exciton in bulk semiconductors, although couplings to phonons are widely investigated,[54] the explicit expression for the Huang-Rhys parameter is not given as far as we know. In this appendix we calculate the Huang-Rhys factor for a Wannier exciton in bulk semiconductors. The exciton–phonon-matrix element for the bulk is given by,

$$v(k)=\int_0^\infty d^3r\,\phi_{1s}^*(r)\phi_{1s}(r)(e^{i\mathbf{k}\cdot t_2\mathbf{r}}-e^{-i\mathbf{k}\cdot t_1\mathbf{r}}) \tag{A1}$$

where

$$t_1=\frac{m_1^*}{m_1^*+m_2^*} \quad \text{and} \quad t_2=\frac{m_2^*}{m_1^*+m_2^*},$$

and we use the hydrogenlike wave function for the exciton state as

$$\phi_{1s}(r)=\left[\frac{1}{\pi a_B^3}\right]^{1/2} e^{-r/a_B}. \tag{A2}$$

The integral in (A1) can be analytically performed,

$$v(\mathbf{k})=\frac{16}{[(ka_Bt_1)^2+4]^2}-\frac{16}{[(ka_Bt_2)^2+4]^2}. \tag{A3}$$

Finally, we obtain g from substituting (A3) in (8),

$$\begin{aligned} g&=\frac{f_0^2}{2\pi^2(\hbar\omega_{\mathrm{LO}})^2}\int_0^\infty dk\,|v(k)|^2 \\ &=\frac{f_0^2}{32\pi a_B(\hbar\omega_{\mathrm{LO}})^2} \\ &\quad\times\frac{(m_1^*-m_2^*)^2(5m_1^{*2}+14m_1^*m_2^*+5m_2^{*2})}{m_1^*m_2^*(m_1^*+m_2^*)^2}. \end{aligned} \tag{A4}$$

Since g depends largely on the choice of the effective masses as shown in (A4), we calculate g with $m_2^*=0.45$, 0.68, and 1.0 for CdSe and obtain $g=0.38$, 0.79, and 1.4, respectively. For GaAs we use $m_2^*=\gamma_1^{-1}=0.146$ and obtain $g=0.0079$.

[1] Al. L. Efros and A. L. Efros, Fiz. Tekh. Poluprovodn. **16**, 1209 (1982) [Sov. Phys. Semicond. **16**, 772 (1982)].
[2] L. E. Brus, IEEE J. Quantum Electron. **22**, 1909 (1986).
[3] L. E. Brus, J. Chem. Phys. **79**, 5566 (1983).
[4] L. E. Brus, J. Chem. Phys. **80**, 4403 (1984).
[5] Y. Kayanuma, Solid State Commun. **59**, 405 (1986).
[6] S. V. Nair, S. Sinha, and K. C. Rustagi, Phys. Rev. B **35**, 4098 (1987).
[7] P. E. Lippens and M. Lanoo, Phys. Rev. B **41**, 6079 (1990).
[8] Y. Kayanuma and H. Momiji, Phys. Rev. B **41**, 10 261 (1990).

[9]E. Hanamura, Phys. Rev. B **37**, 1273 (1988).
[10]T. Takagahara, Phys. Rev. B **36**, 9293 (1987).
[11]L. Banyai, Y. Z. Hu, M. Lindberg, and S. W. Koch, Phys. Rev. B **38**, 8142 (1988).
[12]R. K. Jain and R. C. Lind, J. Opt. Soc. Am. **73**, 647 (1983).
[13]S. S. Yao, C. Karaguleff, A. Gabel, R. Fortenberry, C. T. Seaton, and G. I. Stegeman, Appl. Phys. Lett. **46**, 801 (1985).
[14]S. Schmitt-Rink, D. A. B. Miller, and D. S. Chemla, Phys. Rev. B **35**, 8113 (1987).
[15]L. Katsikas, A. Eychmüller, M. Giersig, and H. Weller, Chem. Phys. Lett. **172**, 201 (1990).
[16]R. Rosseti, S. Nakahara, and L. E. Brus, J. Chem. Phys. **79**, 1086 (1983).
[17]A. P. Alivisatos, T. D. Harris, P. J. Carroll, M. L. Steigerwald, and L. E. Brus, J. Chem. Phys. **90**, 3463 (1989).
[18]P. Roussignol, D. Ricard, C. Flytzanis, and N. Neuroth, Phys. Rev. Lett. **62**, 312 (1989).
[19]M. G. Bawendi, W. L. Wilson, L. Rothberg, P. J. Carroll, T. M. Jedju, M. L. Steigerwald, and L. E. Brus, Phys. Rev. Lett. **65**, 1623 (1990).
[20]T. Itoh and M. Furumiya, J. Lumin. **48&49**, 704 (1991).
[21]A. Uhrig, L. Banyai, Y. Z. Fu, S. W. Koch, S. Gaponenko, N. Neuroth, and C. Klingshirn, in *Proceedings of the 20th International Conference on the Physics of Semiconductors,* edited by E. M. Anastassakis and J. D. Joannopoulos (World Scientific, Singapore, 1990), p. 2395.
[22]G. D. Mahan, *Many-Particle Physics* (Plenum, New York, 1981).
[23]M. C. Klein, F. Hache, D. Ricard, and C. Flytzanis, Phys. Rev. B **42**, 11 123 (1990).
[24]S. Nomura and T. Kobayashi, Solid State Commun. **73**, 425 (1990).
[25]S. Nomura and T. Kobayashi, Solid State Commun. **74**, 1153 (1990).
[26]K. Huang and A. Rhys, Proc. R. Soc. London Ser. A **204**, 406 (1950).
[27]V. L. Alperovich, V. M. Zaletine, A. F. Kravchenko, and A. S. Terekhov, Phys. Status Solidi B **77**, 465 (1976).
[28]J. Lee, E. S. Koteles, and M. O. Vassel, Phys. Rev. B **33**, 5512 (1986).
[29]H. N. Spector, J. Lee, and P. Melman, Phys. Rev. B **34**, 2554 (1986).
[30]S. Rudin and T. L. Reinecke, Phys. Rev. B **41**, 3017 (1990).
[31]N. C. Constantinou and B. K. Ridley, Phys. Rev. B **41**, 10 622 (1990); **41**, 10 627 (1990).
[32]*Chronological Scientific Tables,* edited by the National Astronomical Observatory (Maruzen, Tokyo, 1989).
[33]J. Bardeen and W. Shockley, Phys. Rev. **80**, 72 (1950).
[34]H. Y. Fan, Phys. Rev. **82**, 900 (1951); Y. P. Varshni, Physica **34**, 149 (1967).
[35]*Landolt-Börnstein Numerical Data and Functional Relationship in Science and Technology,* edited by K. H. Hellwege, New Series, Group X, Vols. 17a and 17b (Springer, Berlin, 1982).
[36]H.D. Vasileff, Phys. Rev. **105**, 441 (1957).
[37]J. Voigt, F. Spielgelberg, and M. Senoner, Phys. Status Solidi B **91**, 189 (1979).
[38]D. A. B. Miller, D. S. Chemla, T. C. Damen, A. C. Gossard, W. Wiegmann, T. H. Wood, and C. A. Burrus, Phys. Rev. B **32**, 1043 (1985).
[39]D. A. B. Miller, D. S. Chemla, and S. Schmitt-Rink, Appl. Phys. Lett. **52**, 2154 (1988).
[40]F. Hache, D. Ricard, and C. Flytzanis, Appl. Phys. Lett. **55**, 1504 (1989).
[41]Y. Wang, A. Suna, J. McHugh, E. F. Hilinski, P. A. Lucas, and R. D. Johnson, J. Chem. Phys. **92**, 6927 (1990).
[42]A. P. Alivisatos, A. L. Harris, N. J. Levinos, M. L. Steigerwald, and L. E. Brus, J. Chem. Phys. **89**, 4001 (1988).
[43]S. A. Moskalenko, M. I. Shmiglyuk, and B. I. Chenik, Fiz. Tverd. Tela (Leningrad) **10**, 351 (1968) [Sov. Phys. Solid State **10**, 279 (1968)].
[44]M. Babiker, J. Phys. C **19**, 683 (1986).
[45]Recently R. Enderlein [Phys. Rev. B **43**, 14 513 (1991)] developed a macroscopic theory of optical phonons in superlattices. He applied the Hermiticity condition and the Bloch condition for solving eigenvalue problems of phonon modes without any particular conditions at interfaces and showed that discontinuities of the displacement may arise at the interface. Then our boundary condition (23) may be too strict, and a theory to describe phonons in microcrystallites in Enderlein's manner needs to be developed. However, because the exciton wave function has vanishing amplitude at the interface, the exciton–interface-phonon coupling remains small.
[46]Jian-Bai Xia, Phys. Rev. B **40**, 8500 (1989).
[47]E. O. Kane, J. Phys. Chem. Solids **1**, 249 (1957).
[48]A. Baldereschi and N. O. Lipari, Phys. Rev. B **8**, 2697 (1973).
[49]S. Nomura and T. Kobayashi, Solid State Commun. **78**, 677 (1991).
[50]H. Jahne and E. Gutsche, Phys. Status Solidi **21**, 57 (1967).
[51]H. Haken, Nuovo Cimento **10**, 1230 (1956).
[52]C. B. Duke and G. D. Mahan, Phys. Rev. **139**, A1965 (1965).
[53]R. Merlin, G. Güntherodt, R. Humphreys, M. Cardona, R. Suryanarayanan, and F. Holtzberg, Phys. Rev. B **17**, 4951 (1978).
[54]See, for example, *Excitons,* edited by K. Cho, Topics in Current Physics Vol. 14 (Springer, Berlin, 1979) and G. P. Srivastava, *The Physics of Phonons* (Hilger, Bristol, 1990).